ELSEVIER

Journal of Photochemistry and Photobiology A: Chemistry 154 (2003) 179–188

Journal of Photochemistry and Photobiology A:Chemistry

www.elsevier.com/locate/jphotochem

The novel use of NMR spectroscopy with in situ laser irradiation to study azo photoisomerisation

Katrina M. Tait [a], John A. Parkinson [a,1], Simon P. Bates [b], Warren J. Ebenezer [c], Anita C. Jones [a,*]

[a] *Department of Chemistry, University of Edinburgh, West Mains Road, Edinburgh EH9 3JJ, UK*
[b] *Department of Physics and Astronomy, University of Edinburgh, Mayfield Road, Edinburgh EH9 3JZ, UK*
[c] *DyStar UK Ltd., Earl Road, Cheadle Hulme, Cheshire SK8 6GH, UK*

Received 11 July 2002; received in revised form 19 August 2002; accepted 9 September 2002

Abstract

Cis–trans photoisomerisation of four azo dyes has been studied by ^{1}H nuclear magnetic resonance (NMR) spectroscopy, with in situ laser irradiation of the sample. The laser radiation was coupled into the sample within the NMR magnet via an optical fibre. This enabled the first ^{1}H NMR measurements to be made of the transient *cis* isomers of 4-(4-nitrophenylazo)aniline (CI Disperse Orange 3) and 4-[*N*-ethyl-*N*-(2-hydroxyethyl)amino]-4′-nitroazobenzene (CI Disperse Red 1). Typical NMR methods, including ^{1}H 1D, ^{1}H–^{1}H 2D COSY and ^{1}H–^{1}H 2D EXSY/NOESY, were used to assign ^{1}H resonances of the *trans* and *cis* isomers. Ab initio calculations were used to predict the chemical shifts of *cis*- and *trans*-azobenzene, in good agreement with the experimental results, and to rationalise the chemical shift changes observed on isomerisation.

Keywords: Azo dye; Photoisomerisation; *Cis–trans* isomerisation; NMR spectroscopy; Laser irradiation

1. Introduction

Azo dyes constitute the most important class of dyestuff. The behaviour of azo dyes under irradiation with visible light is an important parameter which determines their potential usefulness. Thus, understanding the photochemistry and resultant properties of azo dyes is an important goal. Despite much previous work in this area [1–8] little is understood about the molecular processes leading to visible effects such as bleaching or colour change (photochromism). This is partly due to the difficulties associated with interpreting data from analytical techniques currently used to study photofading. Generally, previous work on the reversible photoisomerisation of azo dyes has employed UV-Vis spectroscopy, which gives little information about the *cis* isomers so formed. We report here the use of nuclear magnetic resonance (NMR) spectroscopy combined with in situ laser irradiation of the sample, as an alternative, powerful spectroscopic technique for probing the photochromism of azo dyes.

This work seeks to demonstrate the effectiveness of this technique by studying the *cis–trans* isomerisation of some simple mono-azo dyes, namely azobenzene and three of its derivatives, 4-dimethylaminoazobenzene (Methyl Yellow), 4-(4-nitrophenylazo)aniline (CI Disperse Orange 3), and 4-[*N*-ethyl-*N*-(2-hydroxyethyl)amino]-4′-nitroazobenzene (CI Disperse Red 1). The molecular structures are shown in Scheme 1. For these dyes, previous studies indicate that the predominant photochemical process is *cis–trans* isomerisation. The *trans* isomer is thermally the more stable species and upon irradiation, by either UV or visible light, a photostationary state (PSS) is attained consisting of *cis* and *trans* isomers. The reverse process, *cis* to *trans* isomerisation, is induced both photochemically and thermally [7,8]. Whereas *cis*-azobenzene and *cis*-Methyl Yellow are moderately stable at room temperature ($t_{1/2}$ = 119 h at 25 °C [9] and, $t_{1/2}$ = 21 min at 19 °C [9], respectively), *cis*-Disperse Orange 3 and *cis*-Disperse Red 1 are unstable ($t_{1/2}$ = 1 s [6], and $t_{1/2}$ = 0.65 s [6], at 20 °C, respectively). To enable the spectroscopic observation of these short-lived isomers, an optical fibre was used to deliver light from a CW argon/krypton laser directly into the sample inside the NMR magnet. Continuous laser irradiation of the sample solution during NMR

* Corresponding author.
E-mail address: a.c.jones@ed.ac.uk (A.C. Jones).
[1] Present address: Department of Pure and Applied Chemistry, University of Strathclyde, 295 Cathedral Street, Glasgow G1 1XL, UK.

1010-6030/03/$ – see front matter © 2003 Elsevier Science B.V. All rights reserved.
PII: S1010-6030(02)00347-7

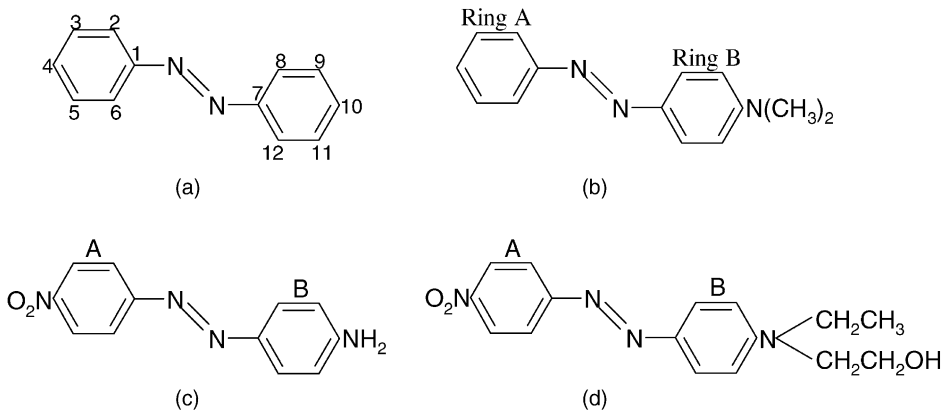

Scheme 1. Structures of the dyes studied: (a) azobenzene; (b) Methyl Yellow; (c) Disperse Orange 3; (d) Disperse Red 1. The atom numbering system shown for azobenzene is used for all dyes.

data acquisition maintains the concentration of transient species.

The geometrical isomerisation of azobenzene and related molecules has been studied extensively using both UV and visible irradiation [1–8]. In all previous work, analysis of the isomerisation process has been carried out by UV-Vis absorption spectroscopy. Despite the advantage of high sensitivity, this technique is limited by poor resolution and curve-fitting techniques must be employed to separate the overlapping spectra of the two isomers. In contrast, the NMR spectra of the *cis* and *trans* isomers are well resolved and can be unambiguously identified.

In addition to demonstrating the effectiveness of NMR spectroscopy in monitoring the photoisomerisation process, we show that the structural information implicit in the NMR spectrum can be used successfully in conjunction with ab initio calculations to determine the molecular geometry of *cis* and *trans* isomers.

2. Experimental

2.1. Materials

The azo dyes, supplied by Aldrich Ltd., were at least 95% pure and were used without further purification. All NMR experiments were carried out in d_6-benzene (99.6 at.% D). Screw capped NMR tubes (528-TR-7) were supplied by Wilmad.

2.2. NMR spectroscopy

NMR spectra were acquired at 298 K (unless otherwise stated) using a Bruker DMX 500 NMR spectrometer operating at 500.13 MHz (^{1}H) equipped with a triple resonance TBI [^{1}H, ^{13}C, X] probehead fitted with an actively shielded *z*-gradient coil for delivering pulsed field gradients.

1D ^{1}H NMR data were acquired typically over 6 kHz centred at 4.5 ppm into 36 000 data points (acquisition time = 3 s) using a standard single pulse-acquire pulse sequence. For 10 mM samples, eight scans were generally sufficient to give a spectrum with good signal-to-noise ratio, giving a total data acquisition time of approximately 60 s. For more dilute samples, typically 512 scans were required to give a similar signal-to-noise ratio, resulting in a total data acquisition time of approximately 20 min. WET solvent suppression [10] was employed for the study of Methyl Yellow. Data were processed using a line broadening function of 0.2 Hz prior to Fourier transformation and phase correction.

2D ^{1}H–^{1}H DQFCOSY and EXSY/NOESY data sets were acquired typically with 32 scans into 1024 data points (FID acquisition time 0.3 s) over a frequency width of 6 kHz centred at 4.5 ppm for each of 512t_1 increments (final digital resolution in F1 was therefore 5.86 Hz/pt). Absolute value (COSY) data were processed using a sine squared window function prior to Fourier transformation in both F1 and F2. Phase sensitive (EXSY/NOESY) data were processed using a squared cosine window function prior to Fourier transformation. For the 2D ^{1}H–^{1}H EXSY/NOESY spectrum presented here, 1 s was allowed for mixing. All data were processed using Xwinnmr (version 2.0, Bruker UK Limited) running on a Silicon Graphics Indigo^2 XZ workstation under Irix 6.2.

2.3. Laser irradiation

The laser source was a continuous wave argon/krypton mixed gas laser (Coherent INNOVA 70 C), giving lines at 676, 647, 568, 530, 520, 514, 488 and 457 nm. The output of the laser was coupled into an optical fibre (FT-600-UMT, Ø 600 μm: Elliot Scientific Ltd.) to deliver light directly into the NMR sample within the probe of the magnet. The end section of the fibre was securely attached to the screw-capped NMR tube via an O-ring seal, with the tip of the fibre lying a few millimetres above the surface of the sample solution. The fibre and the attached tube were then lowered into the magnet. In all experiments, the laser output

power from the fibre was adjusted to 30 mW (measured using a power meter prior to attachment of the NMR tube).

2.4. Quantum chemical calculations

Molecular orbital calculations were carried out with the GAUSSIAN98 program package. Density functional theory calculations (using Becke's 3-parameter exchange functional [11] and the Lee–Yang–Parr correlation functional [12,13] were used, together with the 6-311 + G(2d, 2p) basis set to fully optimise molecular structures. A frequency calculation was carried out to verify that the optimised structure was a global minimum on the potential energy surface. NMR shielding tensors were computed using the (default) Gauge independent atomic orbital (GIAO) method [14] using the same model chemistry of B3LYP/6-311+G(2d, 2p). Chemical shift calculations give only absolute values; we report shifts relative to the de facto standard of the methyl singlet of tetramethylsilane (TMS) at 0 ppm.

3. Results

UV-Vis absorption spectra were recorded for all four dyes and were in good agreement with previously published data [1,6–8]. The spectra show that 457 nm is a suitable laser wavelength to induce photoisomerisation in all cases. Azobenzene has only a weak absorption, $\varepsilon = 270\,\mathrm{mol^{-1}\,l\,cm^{-1}}$, at this wavelength, due to the n–π* transition. For the other three dyes the intense π–π* transition falls in this wavelength region, giving molar absorption coefficients of $\geq 8000\,\mathrm{mol^{-1}\,l\,cm^{-1}}$. In the NMR experiments, the absorbance of the solution was adjusted to allow the laser radiation to penetrate to sufficient depth in the sample to induce photoisomerisation in the NMR probe volume. Thus, for azobenzene a concentration of 10 mM was used, while a 100 μM was used for the other three dyes.

3.1. Azobenzene

As shown in Fig. 1(a), the 1D ^{1}H NMR spectrum of azobenzene, prior to irradiation, consists of a doublet of intensity 4 at 8.02 ppm (corresponding to protons at positions 2/6 and 8/12), a triplet of intensity 2 at 7.09 ppm (positions 4 and 10) and a triplet of intensity 4 at 7.17 ppm, slightly obscured by the solvent peak (positions 3/5 and 9/11).

It is widely accepted that, at thermal equilibrium, azobenzene exists predominantly as the *trans* isomer [7,8]. The NMR spectrum is consistent with this expectation in showing three sets of resonances, corresponding to protons at positions 4, 3/5 and 2/6. Rapid rotation about the N–C1 bond makes protons at positions 2/6 equivalent and protons at positions 3/5 equivalent. The two phenyl rings are chemically and magnetically equivalent, each producing exactly the same set of resonances. The effects of ^3J coupling result in the observed splitting patterns: the signal for the protons

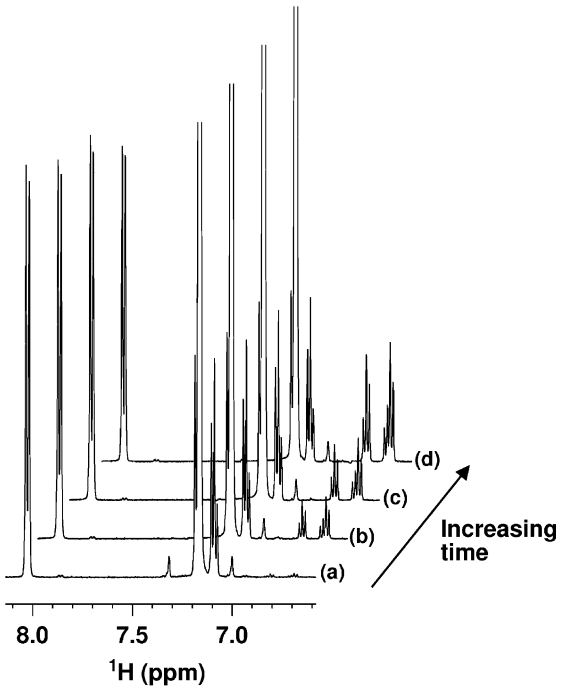

Fig. 1. 1D ^{1}H NMR spectra of azobenzene, (a) prior to irradiation and after (b) 8 min, (c) 12 min and (d) 120 min of continuous irradiation at 457 nm. All data were recorded at 298 K.

at positions 4 and 10 is a triplet of intensity 2; the signal for the protons at positions 3/5 and 9/11 is a triplet of intensity 4; the signal for the protons at positions 2/6 and 8/12 is a doublet of intensity 4.

Fig. 1(b)–(d) shows the ^{1}H NMR spectra of azobenzene recorded after 8, 12, and 120 min of continuous irradiation at 457 nm. As the irradiation proceeds, the signals due to the *trans* isomer decrease in intensity. The weak signals below 7.20 ppm simultaneously grow in intensity. These signals are associated with the *cis* form of azobenzene. Previously reported low-resolution NMR spectra of azobenzene, recorded before [15,16] and after irradiation [16], are consistent with the spectra presented here.

The ^{1}H NMR spectrum of *cis*-azobenzene is expected to contain a set of signals identical in pattern to that of *trans*-azobenzene, but with different chemical shifts. This is consistent with our observations. The new signals which appear upon laser irradiation can be assigned to the *cis* isomer as follows: a triplet of intensity 2 resonating at 6.70 ppm corresponds to protons at positions 4 and 10; a triplet of intensity 4 resonating at 6.81 ppm corresponds to protons at positions 3/5 and 9/11; a doublet resonating at 6.68 ppm corresponds to protons at positions 2/6 and 8/12. The assignments are summarised in Table 1. The composition of the PSS at 457 nm was determined, from peak integrals, to be 25% *cis* isomer.

The ^{1}H NMR spectra of a previously irradiated sample of azobenzene at 323 K, recorded 0, 6, 10, and 50 h after the laser irradiation had been terminated (Fig. 2) show that the peaks attributable to the *cis* isomer decrease in intensity until

Table 1
Assignments of ^{1}H chemical shifts of the *cis* and *trans* isomers of azobenzene, Methyl Yellow, Disperse Orange 3 and Disperse Red 1

Position	Azobenzene $\delta(^1H)$ (ppm)		Methyl Yellow $\delta(^1H)$ (ppm)		Disperse Orange 3 $\delta(^1H)$ (ppm)		Disperse Red 1 $\delta(^1H)$ (ppm)	
	Trans	*Cis*	*Trans*	*Cis*	*Trans*	*Cis*	*Trans*	*Cis*
2/6	8.02	6.68	8.17	6.89	7.64	6.35	7.74	6.47
3/5	7.17	6.81	7.24	6.98	7.89	7.62	7.94	7.71
4	7.09	6.70	7.10	6.82	–	–	–	–
8/12	8.02	6.68	8.23	6.15	7.96	6.77	8.13	6.99
9/11	7.17	6.81	6.46	6.10	6.12	5.82	6.44	6.09
10	7.09	6.70	–	–	–	–	–	–
$(CH_3)_2$	–	–	2.35	2.23	–	–	–	–
NH_2	–	–	–	–	2.94	2.73	–	–
$CH_2\mathbf{CH_3}$	–	–	–	–	–	–	0.75	0.66
$\mathbf{CH_2}CH_3$	–	–	–	–	–	–	3.17	3.08
$\mathbf{CH_2CH_2}OH$[a]	–	–	–	–	–	–	2.89	2.78

[a] The methylene resonances from the alcohol group overlap closely and are treated as one.

the sample becomes 100% *trans*-azobenzene. Although the intensities of the *trans* resonances also appear to decrease, signal integration reveals that all of the *cis* isomer reverts thermally to the *trans* isomer after ~50 h at 323 K. (The loss of signal intensity was due to a loss of magnetic field homogeneity over the course of the lengthy experiment.) The half life of *cis*-azobenzene was found to be 7.75 h at 323 K, measured over four half lives. This is considerably greater than the value of 2.5 h at 329 K, reported by Hartley [9]. However, the latter value, recorded by absorption spectroscopy in 1938, is likely to be an underestimate because of the limited sensitivity of detection of the *cis* isomer.

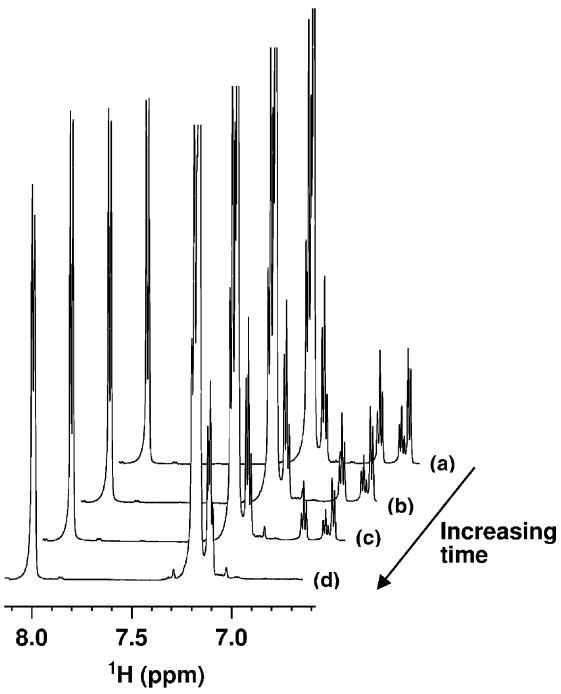

Fig. 2. 1D ^{1}H NMR spectra of a sample of azobenzene, previously irradiated to the PSS at 457 nm, after (a) 0 h, (b) 6 h, (c) 10 h and (d) 50 h of darkness. All data were recorded at 323 K.

3.2. Disperse Red 1

3.2.1. 1D ^{1}H NMR spectroscopy

Asymmetric substitution at the 4 and 10 positions of Disperse Red 1 renders the two aromatic rings magnetically and chemically non-equivalent. Using the same principles as described for azobenzene, protons at positions 2/6 are equivalent and protons at positions 3/5 are equivalent. Similar arguments apply to protons at positions 8/12 and 9/11, giving four pairs of non-equivalent protons. The absence of protons at the 4 and 10 positions reduces the multiplicity of the 3/5 and 9/11 protons from triplets to doublets (ortho coupling = 9 Hz). As with azobenzene, the signals from the *cis* isomer are expected to have chemical shifts different from those of the *trans* isomer. Consequently, the expected resonances for each isomer are four doublets of equal intensity.

The lower concentration used here, compared to that of azobenzene, necessitated a longer spectral acquisition time to achieve a reasonable signal-to-noise ratio. Consequently, it was not possible to acquire spectra sufficiently quickly to monitor the approach to the PSS, which was reached in less than 30 s. Similarly, the thermal *cis* → *trans* reaction rate is so rapid that the progress of this process could not be monitored. Therefore, the following procedure was adopted. A ^{1}H NMR spectrum of the sample was recorded prior to laser irradiation; the sample was then irradiated for a period sufficient to allow the PSS to be attained, after which a spectrum was recorded while maintaining laser irradiation. The sample was then left in darkness for a period of time sufficient to allow complete reversal of the sample to its original composition, after which another spectrum was recorded in darkness. Fig. 3 shows the 1D ^{1}H NMR spectrum of a 100 μM sample of Disperse Red 1, (a) prior to irradiation, and (b) after attainment of the PSS. The differences in the spectra clearly reveal a photochemical conversion. Fig. 3(b) shows that the irradiation has caused a decrease in the intensity of all resonances present in Fig. 3(a), and the appearance of new signals attributable to the *cis* isomer, which essentially replicate the signals observed in Fig. 3(a) but displaced to

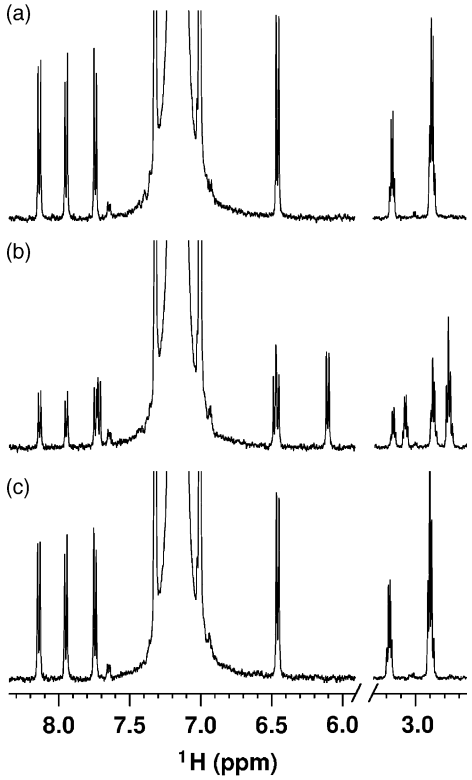

Fig. 3. 1D ^{1}H NMR spectra of Disperse Red 1, (a) prior to irradiation, (b) at the 457 nm PSS, (c) after exposure of the PSS to 30 min of darkness. All data were recorded at 298 K.

higher field. One aromatic signal appears to be missing, but it is almost certainly hidden behind the solvent peak. The apparent triplet at 6.44 ppm is the result of two overlapping doublets. Fig. 3(c) reveals that the process is completely reversible when irradiation is ceased. The spectrum of the *trans* isomer is in good agreement with that reported previously [17].

Despite the reduced number of protons, the 1D ^{1}H NMR spectrum of Disperse Red 1 is made more complex by the fact that all four sets of aromatic resonances of each isomer are identical in intensity and multiplicity. The only distinguishing feature is the frequency at which the protons resonate. Consequently, an assignment of these signals is impossible without recourse to more sophisticated NMR spectroscopy, as presented below. In contrast, the assignment of the amino proton resonances is possible from an inspection of the 1D ^{1}H NMR spectra. The CH_3 group of the ethyl group (a triplet) was found to resonate at 0.75 ppm (data not shown). The adjacent CH_2 (a quartet) resonates at 3.17 ppm (Fig. 3(a)). The methylene proton resonances of the hydroxyethyl group (two triplets) marginally overlap each other (pseudo-quartet at 2.89 ppm). The relative intensity of the two multiplets (2H at 3.17 ppm and 4H at 2.89 ppm) aids the assignment. The chemical shifts of the two triplets are almost identical, signifying that the electronic environments of the CH_2 groups in the hydroxyethyl group unit are very similar. This is a result of N and O having similar electron withdrawing effects. The new multiplets, which appear at 2.78 ppm and 3.08 ppm after irradiation (Fig. 3(b)), are exact replicas of the signals described in Fig. 3(a). A new triplet (CH_3) is also evident, at 0.66 ppm (data not shown).

From peak integrals, it was found that at 457 nm the PSS composition of Disperse Red 1 is 46% *cis* isomer.

3.2.2. 2D ^1H–^1H COSY NMR spectroscopy

1D NMR experiments on Disperse Red 1 were feasible at a concentration of 100 μM but 2D NMR experiments required a higher concentration of dye to overcome sensitivity problems and achieve reasonable data accumulation times. Therefore, a dye concentration of 1 mM was used in combination with a wavelength of 568 nm (chosen from the available laser lines) to maintain effective laser beam penetration. The aromatic region of the 1D ^{1}H and the 2D ^{1}H–^{1}H COSY NMR spectrum of Disperse Red 1 (Fig. 4) were recorded while irradiating the sample at 568 nm (a sufficient period of laser irradiation was allowed for PSS formation prior to NMR data accumulation).

Signals h, g, f and b (Fig. 4) are those present prior to irradiation. Cross-peak [a] correlates h and b. Cross-peak [b] correlates g and f. Signals h and b therefore originate from one ring of the *trans* isomer while signals g and f originate from the other ring of the same isomer.

The photo-induced signals are e, d, c and a. Signal e correlates with c, signified by cross-peak [c], and so e and c originate from the same ring. Signal a correlates through cross-peak [d] to d, which is only just observable behind

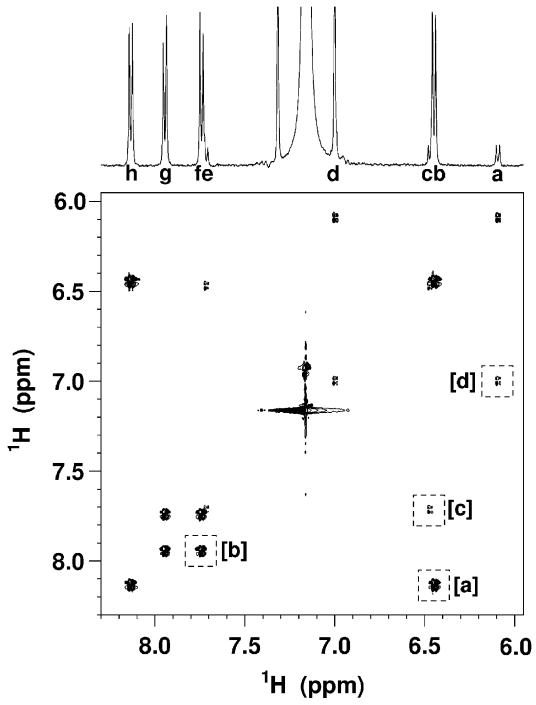

Fig. 4. 1D ^{1}H NMR spectrum and 2D ^{1}H–^{1}H COSY NMR spectrum of Disperse Red 1 (1 mM) at the 568 nm PSS, at 298 K.

one of the ^{13}C satellite signals of the solvent. Resonances a and d originate, therefore, from the remaining ring and d is thus the signal originally thought to be missing. One of the many advantages of 2D NMR is highlighted by the fact that d can be observed despite the fact that it is mostly hidden by the ^{13}C satellite signal of the solvent.

3.2.3. 2D ^1H–^1H EXSY/NOESY NMR spectroscopy

Whereas COSY NMR spectroscopy involves the through bond correlation of neighbouring protons in the same molecule, exchange spectroscopy visualises the magnetisation transfer pathway between protons on two or more unique molecular species in chemical exchange with one another. Thus, when the chemical exchange (in this case between two geometrical isomers) is slow enough on the NMR time scale, off diagonal exchange cross-peaks will be observed between protons originating from different species. The pulse sequence used to obtain an EXSY NMR spectrum is identical to the 2D NMR technique used to obtain nOe data (NOESY), which gives information about through space correlations. In this case not only does the technique map the magnetisation transfer between the two isomers via exchange spectroscopy, but it also supplies through space correlations essential to the assignment. The diagonals of 2D NOESY spectra are, by convention, phased negatively. Small molecules with fast tumbling times (those studied here) produce nOe cross-peaks opposite in sign to the diagonal (i.e. nOes are positive). In contrast, EXSY cross-peaks appear as the same sign as the diagonal, i.e. negative, therefore allowing the two types of cross-peaks to be distinguished.

The 1D ^1H and the 2D ^1H–^1H EXSY NMR spectra for Disperse Red, including the aromatic and aliphatic regions, are shown in Fig. 5. The two sets of overlapping triplets, centred at 2.89 and 2.78 ppm of the 1D ^1H NMR spectrum, are globally labelled j and i, respectively.

In the aromatic region, two EXSY cross-peaks are observed: [a] shows the presence of chemical exchange between protons assigned to resonances a and b; [b] shows that chemical exchange exists between protons assigned to resonances d and h. Thus d and h originate from protons at equivalent positions in both isomers. A similar conclusion can be drawn for a and b.

The positive nOe cross-peak [c] indicates that the protons that give rise to resonance j are closest in space to the protons giving rise to resonance b. Signal j was previously assigned to the methylenes of the hydroxyethylamine group. Thus, b is assigned to protons 9/11 of the *trans* isomer. From the COSY data, signals b and h arise from protons on the same ring; therefore, h can be assigned to protons at positions 8/12 of the *trans* isomer. The chemical exchange cross-peak [a] between a and b allows a to be assigned to protons 9/11 of the *cis* isomer. A COSY correlation between a and c assigns c to protons 8/12 of the *cis* isomer. NOe cross-peaks between all four aliphatic resonances and signals a and b appear at a lower noise threshold (data not shown). Nevertheless,

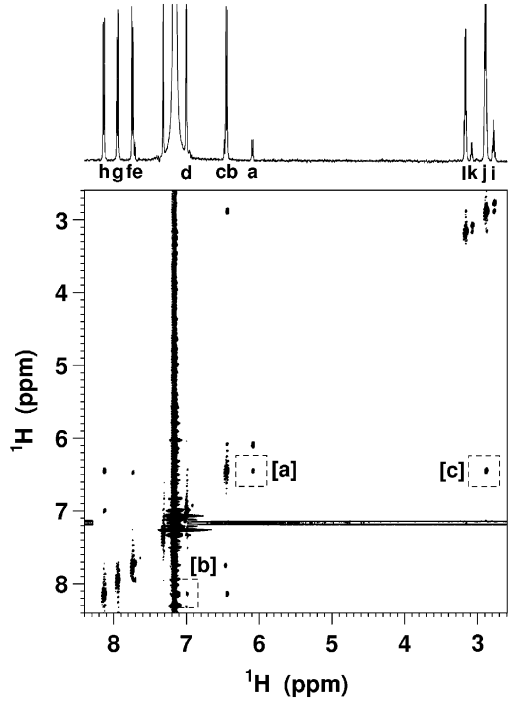

Fig. 5. 1D ^1H NMR spectrum and 2D ^1H–^1H EXSY NMR spectrum of Disperse Red 1 (1 mM) at the 568 nm PSS, at 298 K.

assignment was still possible using exchange cross-peak [a], completing the assignment of all proton resonances for ring B of both the *cis* and *trans* form of Disperse Red 1.

To assign ring A using the experiments described would require nOe information between positions 2/6 and 8/12. Despite a long mixing time (1 s), no such nOe was observed, because the distance between the two rings is greater than 5 Å in both the *cis* and *trans* forms. Nevertheless, it is possible to determine that resonances g and f originate from ring A of the *trans* isomer and that resonances e and c originate from ring A of the *cis* isomer. To complete the assignment it is assumed that, because of the deshielding effect of the NO_2 group at position 4, protons at positions 3/5 in both isomers will resonate at higher frequency than those at 2/6. The assignments of *trans* and *cis* isomers are summarised in Table 1.

From Figs. 4 and 5 it is clear that a different PSS has been reached by irradiating at 568 nm. At this wavelength, the PSS composition is 12% *cis*-Disperse Red 1.

3.3. Methyl Yellow

Ring A of Methyl Yellow is expected to show a doublet and a triplet of intensity 2, and a triplet of intensity 1 (cf. azobenzene). Ring B is expected to show two doublets both of intensity 2 (cf. Disperse Red). Fig. 6(a) shows the 1D ^1H NMR spectrum of a 100 μM sample of Methyl Yellow prior to irradiation. After a period of irradiation sufficient to reach the PSS, and while maintaining irradiation, Fig. 6(b)

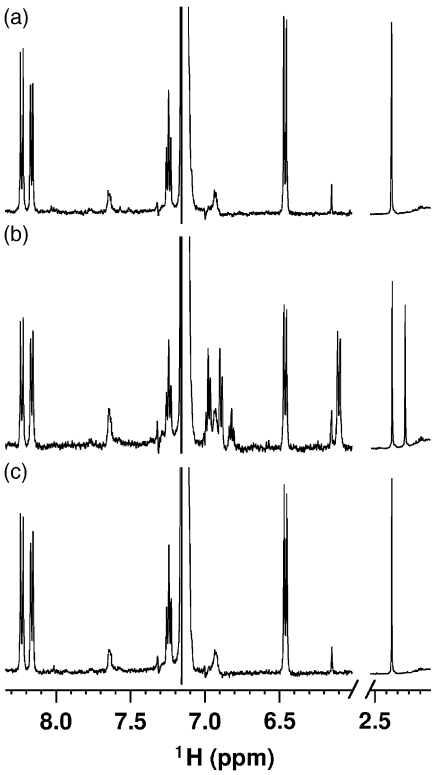

Fig. 6. 1D ^{1}H NMR spectra of Methyl Yellow, (a) prior to irradiation, (b) at the 457 nm PSS, (c) after exposure of the PSS to 30 min of darkness, all at 298 K.

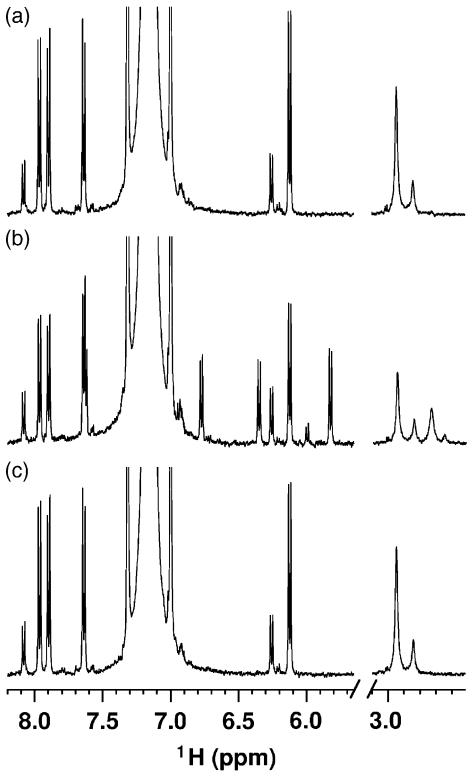

Fig. 7. 1D ^{1}H NMR spectra of Disperse Orange 3, (a) prior to irradiation, (b) at the 457 nm PSS, (c) after exposure of the PSS to 30 min of darkness, all at 298 K.

was recorded. Then, after a period of darkness sufficient to allow the sample to revert to its original composition, Fig. 6(c) was recorded. Spectrum (a) contains the ^{1}H NMR signals expected for the *trans* isomer and spectrum (b) contains the new resonances expected from the formation of the *cis* isomer. The process is completely reversible as shown by Fig. 6(c). 2D COSY and EXSY NMR experiments (data not included) were carried out on a 1 mM sample with irradiation at 520 nm. Information gained from these experiments aided in the assignment of the ^{1}H NMR spectrum shown in Fig. 6(b). In contrast to Disperse Red 1, the proton at position 4 imparts sufficient information to allow assignment of ring A. As before, nOe data facilitated assignment of ring B. The assignments are summarised in Table 1. The composition of the PSS following irradiation at 457 and 520 nm was found to be 66% and 22% *cis* isomer, respectively.

3.4. Disperse Orange 3

The expected resonances for Disperse Orange 3 are four equal intensity doublets (cf. Disperse Red). Fig. 7(a) shows the 1D ^{1}H NMR spectrum of a 100 μM sample of Disperse Orange prior to irradiation. After a period of irradiation sufficient to reach the PSS, and while maintaining irradiation, Fig. 7(b) was recorded. After a period of darkness sufficient to allow the sample to revert to its original composition, Fig. 7(c) was recorded. Spectrum (a) contains the signals expected for the *trans* isomer and spectrum (b) contains the extra resonances expected for the formation of the *cis* isomer. Again the process is completely reversible thermally (Fig. 7(c)). Previous low-field NMR spectra of *trans*-Disperse Orange 3 [15,18] appear to be consistent with the spectra reported here; however, their low resolution precludes a detailed comparison.

2D COSY and EXSY NMR experiments (data not included) were carried out on a 1 mM sample with irradiation at 530 nm. As for Disperse Red 1, these experiments did not provide a complete assignment of the 1D spectra and the deshielding effect of the NO_2 group was invoked to assign the protons of ring A. The assignments are summarised in Table 1. The composition of the PSS of Disperse Orange 3 following irradiation at 457 and 530 nm was 44 and 18% *cis* isomer, respectively.

3.5. Ab initio calculations on azobenzene

Ab initio calculations on azobenzene were undertaken to predict the ^{1}H chemical shifts of the *trans* and *cis* isomers for comparison with the experimental data. The computed structures are shown in Fig. 8. The global minimum structure of the *trans* isomer was found to be planar with C_{2h} symmetry and the structural parameters computed here are essentially identical to those reported in a recent study by

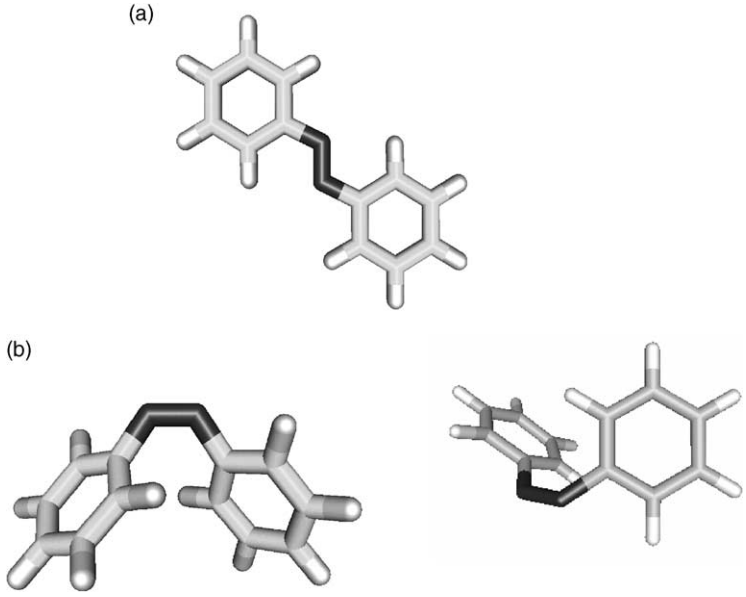

Fig. 8. The calculated minimum energy structures of (a) *trans*-azobenzene and (b) *cis*-azobenzene. Two views of the *cis* isomer are shown, to illustrate the relative orientation of the phenyl rings.

Table 2
Comparison of experimental and calculated chemical shifts for azobenzene

Position	Experimental $\delta(^1H)$ (ppm)		Calculated $\delta(^1H)$ (ppm)		Experimental $\Delta\delta(^1H)$ (ppm)	Calculated $\Delta\delta(^1H)$ (ppm)
	Trans	*Cis*	*Trans*	*Cis*		
2/6	8.02	6.68	8.40	7.04	1.34	1.36
3/5	7.17	6.81	7.83	7.48	0.36	0.35
4	7.09	6.70	7.70	7.35	0.39	0.35

Tsuji et al. [19] and previously by Biswas and Umapathy [20]. *Cis*-azobenzene was found to be non-planar, with C_2 symmetry. Again, the structural parameters are in good agreement with those determined by Biswas and Umapathy, particularly the rotation of the phenyl rings by 56° with respect to the N=N–C plane. The *trans* isomer was calculated to be more stable by 68 kJ mol^{-1}, in agreement with the experimental value of 56 kJ mol^{-1} reported by Shulze et al. [21]. The calculated chemical shifts and differences in shifts between *trans* and *cis* isomers, $\Delta\delta$, are shown in Table 2, in comparison with the experimentally determined values. In the experimental data the pairs of protons 2/6 and 3/5 appear equivalent because of internal rotation of the phenyl group about the C–N bond. In the static computed structure, these protons have different chemical shifts. For comparison with the experimental values, the mean of the calculated shifts for protons 2/6 and 3/5 are given.

4. Discussion

For all four azo dyes, irradiation at 457 nm produces a new species, which can easily be detected and characterised by high field NMR spectroscopy. Assignments of the 1D ^1H NMR spectra show that, in all cases, the photochemical product is the *cis* isomer of the respective dye. The absence of unidentifiable peaks in the NMR spectra and the full reversibility of the photoconversion rule out fragmentation or any other type of photochemical reaction. Unlike the UV-Vis spectra, which overlap strongly, the NMR spectra of the *trans* and *cis* isomers are well-resolved, allowing the composition of the PSS to be determined accurately. The percentages of *cis* isomer present at the PSS for the four dyes, at various wavelengths are summarised in Table 3. It can be seen that there is considerable variation in the composition of the PSS at 457 nm between the

Table 3
Percentage of the *cis* isomer present at the PSS

	457 nm (%)	520 nm (%)	530 nm (%)	568 nm (%)
Azobenzene	25	–	–	–
Methyl Yellow	66	22	–	–
Disperse Orange 3	44	–	18	–
Disperse Red 1	46	–	–	12

different dyes, with azobenzene showing the smallest proportion of *cis* isomer and Methyl Yellow the greatest. A similar trend is apparent in the rather sparse data in the literature from UV-Vis measurements: for azobenzene a PSS composition of 17% *cis* at 436 nm has been reported [3]; for Disperse Red 1, >31% *cis* at 450 nm [6]; and for Methyl Yellow a maximum of 68% *cis* (wavelength not given) [1]. For all four dyes, there is a marked decrease in the proportion of *cis* isomer at longer wavelength, reflecting the increase in relative absorption strength of the *cis* isomer at these wavelengths.

An interesting feature which has emerged from the NMR assignments is the large difference in chemical shifts between proton resonances of *cis* and *trans* isomers, $\Delta\delta$, for protons at positions 8/12. As shown in Table 1, for all four dyes, ^{1}H resonances for protons at positions 8/12 have $\Delta\delta$ values of greater than 1 ppm. By comparison, positions 9/11 (and 10 for azobenzene) show an average $\Delta\delta$ of approximately 0.4 ppm. For azobenzene and Methyl Yellow, where the assignment of ring A is complete, the same large values for $\Delta\delta$ are shown for positions 2/6. The consistency of this feature is so great, that $\Delta\delta$ values can be used to confirm the assignment of ring A for Disperse Red 1 and Disperse Orange 3. Thus, for Disperse Red 1, δ values of 7.74 and 6.47 are assigned to positions 2/6 of the *trans* and *cis* isomer, respectively, and 7.94 and 7.71 to positions 3/5 in *trans* and *cis* forms, respectively. Similarly, for Disperse Orange 3, δ values of 7.64 and 6.35 are assigned to positions 2/6 of the *trans* and *cis* isomers, respectively, and 7.89 and 7.62 to positions 3/5 in *trans* and *cis* forms, respectively.

The chemical shifts predicted for azobenzene by the ab initio calculations are in good agreement with the experimental values, supporting the validity of the computed equilibrium geometries of *cis* and *trans* isomers. The predicted $\Delta\delta$ values are in particularly good agreement with those determined experimentally. Therefore, the computed structures are useful in visualising the change in geometry, which leads to the large shielding of protons adjacent to the azo linkage upon *trans* to *cis* isomerisation. Such changes in observed chemical shifts are anticipated from an empirical standpoint. The change in geometry will result in large effects on chemical shifts for the following reasons: the two aromatic rings are initially remote from one another (*trans*) but encounter one another closely as a result of photoisomerisation (*cis*); protons that were initially only subject to the local *deshielding* effect of their 'own' aromatic ring within the ring plane (*trans* form) now encounter the additional *shielding* effect of the remote out-of-plane aromatic ring (*cis*). In the optimised *cis* structure, the closest distance between the centre of one aromatic ring and the 2/6 protons belonging to the remote aromatic ring is 2.43 Å, corresponding to a 56° angle between the aromatic ring plane and the N=N–C plane. The angle formed between the plane of one aromatic ring and the 2/6 proton closest to it on the remote aromatic ring is also ∼56°. Both the angle and the distance between an aromatic ring and a proton above the plane of the ring are factors that govern the shielding effect experienced by the proton. A location close to and perpendicular to the ring plane results in the largest shielding effects. By comparison a location further away from the centre of the ring and at an angle to the normal of the plane results in smaller, though not inconsiderable effects.

5. Conclusions

For the four azo molecules studied, NMR spectroscopy unambiguously shows the occurrence of photoinduced *trans–cis* isomerisation, the absence of any other photoproducts and the complete thermal reversibility of the isomerisation. The observation of a characteristic, large change in chemical shift between *cis* and *trans* isomers, for protons adjacent to the N=N bond, will be a useful diagnostic tool for isomerisation in more complex azo dyes. For the first time, the NMR spectra of the short-lived *cis* isomers of Disperse Red 1 and Disperse Orange 3 have been recorded, demonstrating the potential of this technique for identifying transient intermediates and unstable products of photochemical reactions. Moreover, the use of NMR data together with ab initio calculations promises to provide valuable structural information on these species.

Acknowledgements

We gratefully acknowledge DyStar UK Ltd. and the EPSRC for funding a CASE studentship for KMT, and Prof. Peter Sadler for NMR and laser instrument time. We also thank Dr. Mike Hutchings for helpful discussions.

References

[1] W.R. Brode, J.H. Gould, G.M. Wyman, J. Am. Chem. Soc. 74 (1952) 4641.
[2] P. P Birnbaum, D.W.G. Style, Trans. Faraday Soc. 50 (1954) 1192.
[3] G. Zimmerman, L. Chow, U. Paik, J. Am. Chem. Soc. 80 (1958) 3528.
[4] S. Malkin, E. Fischer, J. Am. Chem. Soc. 66 (1962) 2482.
[5] P. Bortolus, S. Monti, J. Phys. Chem. 83 (1979) 648.
[6] N.R. King, E.A. Whale, F.J. Davis, A. Gilbert, G.R. Mitchell, J. Mater. Chem. 7 (1997) 625.
[7] J. Griffiths, J. Chem. Soc. Rev. 1 (1972) 481.
[8] J.F. Rabek (Ed.), Photochemistry and Photophysics, vol. 2, CRC Press, Boca Raton, 1990, Chapter 4.
[9] G.S. Hartley, J. Chem. Soc. (1938) 633.
[10] S.H. Smallcombe, S.L. Patt, P.A. Keifer, J. Magn. Reson. 117 (1995) 295.
[11] A.D. Becke, J. Chem. Phys. 98 (1993) 5648.
[12] C. Lee, W. Yang, R.G. Parr, Phys. Rev. B 37 (1998) 785.
[13] B. Miehlich, A. Savin, H. Stoll, H. Preuss, Chem. Phys. Lett. 157 (1989) 200.

[14] K. Wolinski, J.F. Hilton, P. Pulay, J. Am. Chem. Soc. 112 (1990) 8251.
[15] L. Skulski, W. Waclawek, A. Szurowska, Bull. Acad. Polon. Sci., Sér. Sci. Chim. 20 (1972) 463.
[16] L.S. Lever, M.S. Bradley, C.S. Johnson Jr., J. Magn. Reson. 68 (1986) 335.
[17] L.A. Federov, P. Savarino, V.I. Dostovalova, G. Viscardi, R. Carpignano, E. Barni, Magn. Reson. Chem. 29 (1991) 747.
[18] L. Skulska, J. Kleps, Bull. Acad. Polon. Sci., Sér. Sci. Chim. 21 (1973) 859.
[19] T. Tsuji, H. Takashime, H. Takeuchi, T. Egawa, S. Konaka, J. Phys. Chem. A 105 (2001) 9347.
[20] N. Biswas, S. Umapathy, J. Phys. Chem. A 101 (1997) 5555.
[21] F.W. Shulze, H.J. Detrik, H.K. Cammenga, H. Klinge, Z. Physiol. Chem. 107 (1977) 1.